

GEOCHEMICAL FEATURES OF URANIUM-RARE EARTH MINERALIZATION IN BLACK SHALES OF NORTHERN NUROTA RIDGE (ON THE EXAMPLE OF THE USTUK ORE OCCURRENCE)

¹A.A. Khalilov*, ²Z.Y. Ergashov, ³E.H. Kutliev, ⁴N.Z. Gafforova, ⁵A.A. Kushiev, ⁶E.A. Khakkulov

University of Geological Sciences in Tashkent¹

National University of Uzbekistan named after Mirzo Ulugbek²

National University of Uzbekistan named after Mirzo Ulugbek³

Tashkent State Technical University named after Islam Karimov

University of Geological Sciences in Tashkent⁵

JV LLC "Oltin Kon"⁶

**Author for Correspondence: abrorabdulaev1987@gmail.com*

ABSTRACT

With the development of science and technology and the increasing demand for high-tech materials, the need for new raw materials such as rare earth elements (REEs) is rising. To create and enrich the base of REEs, the Ministry of Geology and Mining Industry of the Republic of Uzbekistan is encouraging the search for industrial mineralization of these raw materials in several promising areas. In the black shales of the Central Kyzylkum, particularly in the Northern Nurota ridge, numerous associations of uranium, molybdenum, and vanadium have been studied. Recent exploration and scientific research by several scientists, such as A.A. Khalilov and I.B. Turamuratov, have identified and are studying the relationship between uranium-vanadium-molybdenum mineralization and REE mineralization. This article presents the results of studies of the geochemical properties of these critical metals at the Ustuk ore occurrence.

Keywords: *Northern Nurota Ridge, Black Shale, Uranium, Molybdenum, Vanadium, Rare Earth Elements (Rees), Proterozoic Eon, Geochemical Features.*

INTRODUCTION

The Proterozoic eon, spanning from 2.5 billion to 541 million years ago, was a significant period in Earth's history marked by crucial geological, atmospheric, and biological changes. Among the notable geological formations from this eon are the black shales, sedimentary rocks rich in organic material. These black shales are particularly noteworthy for their high concentrations of uranium, molybdenum, vanadium, and rare earth elements (REEs). Understanding the reasons behind this enrichment involves delving into the geochemical, biological, and depositional processes that occurred during the Proterozoic. The increasing demand for important raw materials such as uranium and rare earth elements makes the study of these black shales urgent. This paper aims to understand the geological, geochemical, and environmental factors contributing to the enrichment of these elements in Proterozoic black shales and to develop criteria for finding large deposits. In preparing this article, the results of previous geological exploration work in the territory and the results of work performed during my activity were used. ICP-MS results (61 elements) from more than 7,000 samples taken from lithochemical surveys, various mine workings (trenches, drill holes, and underground mine workings) were analyzed.

The practical significance of the work lies in the study of the statistical features of the mineralization of uranium and rare earth elements, the connection with satellite elements, the determination of the main associations of mineralization through geostatistical analysis of geochemical data, and the conclusion about their location in space and, ultimately, the development of geochemical search criteria.

Research Article

Black shales are fine-grained sedimentary rocks characterized by high organic carbon content. They typically form in anoxic (oxygen-poor) environments such as deep marine basins or restricted sea areas. The lack of oxygen in these settings allows for the preservation of the concentration of metals and organic matter, which contributes to the dark color of the shales. Organic matter can bind with metals like uranium, molybdenum, and vanadium, facilitating their accumulation. The decomposition of organic matter also releases hydrogen sulfide (H₂S), which can react with metal ions to form insoluble metal sulfides, further concentrating these elements in the shale.

2. Geological Setting

The Ustuk ore occurrence is located in the central part of the Northern Nurota ridge, stretching for more than 100 km in the northwest direction, 7-40 km wide, and administratively belongs to the Koshrabotsky district of the Samarkand region. The central and eastern parts of the area differ from the rest in relative height exceeding 300 m and absolute height reaching 2136 m (Kharchigoy peak). The slopes and western part of the ridge are dry hills with a small number of outcrops of Paleozoic rocks.

The Ustuk ore occurrence is located in the Zarafshano-Turkestan structural-formational zone, on the territory of the Ustuk-Fozilmansky (95 km²) uranium ore field, within the Uchmolo-Ustuk uranium-bearing structural unit, on a watershed with an absolute height of 1600-2114 m (**figure 1**).



Figure 1: Location map of the Ustuk ore occurrence

The northern slope of the Northern Nurota ridge is quite narrow and steep, and its foothills adjoin the Central Kyzylkum Plain. The southern slope is low and wide, forming a steppe zone. The topography of the upper part of the slopes adjacent to the reservoir is very uneven and rocky, with exposures of Paleozoic rocks. Alluvial and colluvial rocks are rare, and Quaternary sediments are scarce. On the southern slope of the central part of the Northern Nurota ridge, waterways such as Nakurtsoy, Ukursaroy, Gudzhumsoy, Navkatsoy, and Pangatsoy flow towards the Zerafshan Valley.

The central and western parts of the Northern Nurota mountain range are composed of Precambrian, Paleozoic, and Cenozoic sediments. The studied field is represented mainly by Precambrian (Uchmola

Research Article

formation - PR1? uc, Suvliksoy formation - R2 sv), Paleozoic (Konsoy formation - O1-2 kn), and eluvial-deluvial Quaternary sediments (**figure 2**).

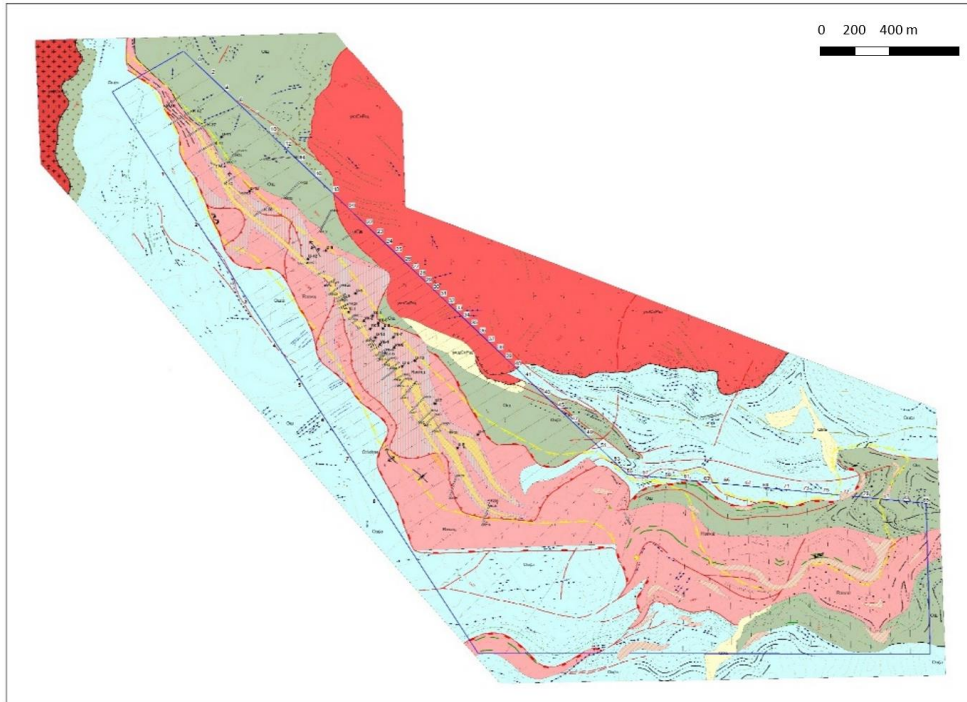


Figure 2: Geological map of the Ustuk ore occurrence

3. Dataset and Methods

Initially, the Ustuk area database was prepared in MS Excel for processing in computer programs. Statistica 10 was used for statistical analysis, QGIS and Surfer 18 were used for geospatial analysis and geochemical mapping.

At the next stage, the samples were divided into **7 groups** based on the definition of rocks in the database, as well as the amount of rock-forming chemical elements:

Table 1: Number of samples used in the study by group

Name of rocks	Code	Number of samples
Quartz-sericite shales (phyllites)	1	1 909
Carbonaceous-siliceous shales, microquartzites and quartzites	2	3 146
Granitoids	3	22
Lamprophyre dikes	4	34
Quartz veins	5	164
Limestones and dolomites	6	157
Metasomatites and skarns	7	1 824
Total:		7 256

Descriptive statistical tables for each group (number of samples, arithmetic mean of metals, median, mode, mode frequency, minimum and maximum counts, upper and lower quartile and percentile counts, variance, standard deviation), local background, minimum anomaly magnitude and Clarke number, based on the highest percentile was calculated based on these parameters.

To draw a preliminary conclusion about the distribution of chemical elements in rocks, the calculated Clark concentrations as a result of descriptive statistical analysis for each rock group were arranged in

Figure 3. Dendrogram showing the relationships of chemical elements common in carbonaceous-siliceous shales, microquartzite, and quartzite

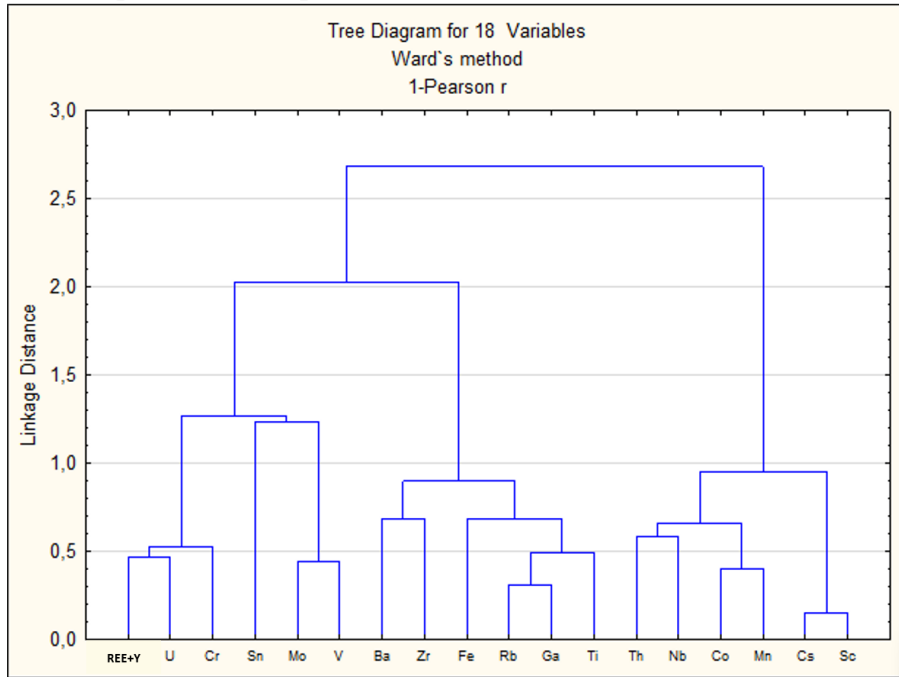


Table 4. Correlation matrix showing the relationship of chemical elements common in metasomatites and skarns

	Sc	Ti	V	Cr	Mn	Fe	Co	Ni	Cu	Ga	Rb	Y	Zr	Nb	Mo	Sn	Cs	La	Ce	Pr	Nd	Sm	Eu	Gd	Tb	Dy	Ho	Er	Tm	Yb	Lu	Th	U	
Sc	1.0	0.0	-0.1	0.8	0.9	-0.1	0.7	0.0	0.0	0.0	0.0	0.0	-0.1	0.4	-0.1	-0.1	0.9	0.0	0.0	0.3	-0.1	-0.1	0.5	-0.1	0.6	-0.1	0.3	-0.1	0.6	-0.1	0.2	0.1	0.0	
Ti	0.0	1.0	-0.1	-0.1	-0.1	0.1	0.1	0.0	0.3	0.4	0.0	0.1	0.7	0.6	0.0	0.2	-0.1	0.2	0.1	0.4	0.4	0.4	0.4	0.3	0.2	0.2	0.1	0.1	0.1	0.2	0.1	0.8	0.0	
V	-0.1	-0.1	1.0	0.1	-0.1	0.2	0.0	0.2	0.0	0.2	0.0	0.3	0.1	0.1	0.5	0.4	-0.1	0.1	0.1	0.5	0.6	0.6	0.4	0.7	0.4	0.7	0.6	0.7	0.5	0.6	0.6	-0.1	0.2	
Cr	0.8	-0.1	0.1	1.0	0.8	-0.1	0.6	0.0	0.0	0.0	0.0	0.1	-0.1	0.4	0.0	0.0	0.6	0.1	0.0	0.4	0.1	0.1	0.5	0.1	0.6	0.1	0.4	0.1	0.6	0.1	0.2	0.1	0.1	
Mn	0.9	-0.1	-0.1	0.8	1.0	-0.1	0.7	0.0	0.0	0.1	0.0	0.0	-0.1	0.4	0.0	0.0	0.8	0.0	0.0	0.3	-0.1	-0.1	0.5	-0.1	0.6	-0.1	0.3	-0.1	0.6	-0.1	0.2	0.1	0.1	
Fe	-0.1	0.1	0.2	-0.1	-0.1	1.0	0.0	0.2	0.1	0.6	0.3	0.1	0.1	0.3	0.4	0.5	-0.1	0.1	0.1	0.1	0.2	0.2	0.0	0.3	0.1	0.3	0.2	0.3	0.1	0.3	0.2	0.1	0.1	
Co	0.7	0.1	-0.1	0.6	0.7	0.0	1.0	0.1	0.1	0.1	0.1	0.1	0.0	0.4	0.0	0.0	0.6	0.0	0.0	0.3	0.0	0.0	0.4	0.0	0.5	0.0	0.2	0.0	0.4	0.0	0.2	0.2	0.1	
Ni	0.0	0.0	0.2	0.0	0.0	0.2	0.1	1.0	0.0	0.1	0.3	0.3	0.1	0.1	0.1	0.2	0.0	0.3	0.4	0.2	0.3	0.2	0.2	0.3	0.2	0.3	0.2	0.3	0.2	0.3	0.2	0.1	0.4	
Cu	0.0	0.3	0.0	0.0	0.0	0.1	0.1	0.0	1.0	0.1	0.0	0.0	0.0	0.2	0.2	0.1	0.0	0.0	0.0	0.2	0.0	0.2	0.3	0.2	0.1	0.0	0.2	0.0	0.0	0.0	0.0	0.0	0.0	
Ga	0.0	0.4	0.2	0.0	0.1	0.6	0.1	0.1	0.1	1.0	0.3	0.1	0.2	0.5	0.3	0.5	0.1	0.1	0.1	0.3	0.3	0.3	0.2	0.3	0.2	0.2	0.2	0.2	0.2	0.2	0.2	0.3	0.1	
Rb	0.0	0.0	0.0	0.0	0.0	0.3	0.1	0.3	0.0	0.3	1.0	0.1	0.0	0.2	0.1	0.2	0.1	0.0	0.2	0.0	0.0	0.0	0.0	0.0	0.0	0.0	0.0	0.0	0.0	0.0	0.0	0.1	0.2	
Y	0.0	0.1	0.3	0.1	0.0	0.1	0.0	0.3	0.0	0.1	0.1	1.0	0.1	0.2	0.1	0.2	0.0	0.7	0.6	0.3	0.4	0.4	0.3	0.4	0.3	0.4	0.4	0.4	0.3	0.5	0.3	0.1	0.3	
Zr	-0.1	0.7	0.1	-0.1	-0.1	0.1	0.1	0.1	0.2	0.0	0.1	1.0	0.4	0.0	0.1	-0.1	0.1	0.2	0.4	0.5	0.5	0.3	0.4	0.2	0.4	0.3	0.4	0.2	0.4	0.4	0.5	0.1	0.1	
Nb	0.4	0.6	0.1	0.4	0.4	0.3	0.4	0.1	0.2	0.5	0.2	0.2	1.0	0.2	0.3	0.3	0.2	0.2	0.6	0.4	0.4	0.5	0.3	0.6	0.3	0.4	0.3	0.5	0.3	0.3	0.6	0.1		
Mo	-0.1	0.0	0.5	0.0	0.0	0.4	0.0	0.1	0.2	0.3	0.1	0.1	0.0	0.2	1.0	0.2	0.0	0.0	0.2	0.2	0.3	0.2	0.3	0.2	0.3	0.3	0.3	0.2	0.3	0.3	-0.1	0.2		
Sn	-0.1	0.2	0.4	0.0	0.0	0.5	0.0	0.2	0.1	0.5	0.2	0.2	0.1	0.3	0.2	1.0	-0.1	0.1	0.1	0.3	0.4	0.4	0.2	0.5	0.3	0.4	0.4	0.4	0.3	0.4	0.4	0.2	0.1	
Cs	0.9	-0.1	-0.1	0.6	0.6	-0.1	0.6	0.0	0.0	0.1	0.1	0.0	-0.1	0.3	0.0	-0.1	1.0	0.0	0.0	0.2	-0.1	-0.1	0.4	-0.1	0.5	-0.1	0.2	-0.1	0.5	-0.1	0.1	0.1	0.0	
La	0.0	0.2	0.1	0.1	0.0	0.1	0.0	0.3	0.0	0.1	0.0	0.7	0.1	0.2	0.0	0.1	0.0	1.0	0.5	0.3	0.3	0.3	0.3	0.3	0.2	0.3	0.2	0.3	0.2	0.3	0.2	0.2	0.1	
Ce	0.0	0.1	0.1	0.0	0.0	0.1	0.0	0.4	0.0	0.1	0.2	0.6	0.2	0.2	0.0	0.1	0.0	0.5	1.0	0.2	0.3	0.3	0.2	0.3	0.2	0.3	0.2	0.2	0.1	0.3	0.2	0.2	0.2	
Pr	0.3	0.4	0.5	0.4	0.3	0.1	0.3	0.2	0.2	0.3	0.0	0.3	0.4	0.6	0.2	0.3	0.2	0.3	0.2	1.0	0.9	0.8	0.9	0.8	0.8	0.7	0.8	0.7	0.7	0.7	0.7	0.5	0.2	
Nd	-0.1	0.4	0.6	0.1	-0.1	0.2	0.0	0.3	0.0	0.3	0.0	0.4	0.5	0.4	0.2	0.4	-0.1	0.3	0.3	0.9	1.0	1.0	0.7	0.9	0.6	0.9	0.7	0.9	0.6	0.8	0.7	0.4	0.2	
Sm	-0.1	0.4	0.6	0.1	-0.1	0.2	0.0	0.2	0.2	0.3	0.0	0.4	0.5	0.4	0.3	0.4	-0.1	0.3	0.3	0.8	1.0	1.0	0.8	1.0	0.6	0.9	0.8	0.9	0.6	0.9	0.8	0.3	0.2	
Eu	0.5	0.4	0.4	0.5	0.5	0.0	0.4	0.2	0.3	0.2	0.0	0.3	0.3	0.5	0.2	0.2	0.4	0.3	0.2	0.9	0.7	0.8	1.0	0.7	0.9	0.7	0.8	0.6	0.8	0.6	0.7	0.4	0.2	
Gd	-0.1	0.3	0.7	0.1	-0.1	0.3	0.0	0.3	0.2	0.3	0.0	0.4	0.4	0.3	0.3	0.5	-0.1	0.3	0.3	0.8	0.9	1.0	0.7	1.0	0.7	1.0	0.9	0.9	0.6	0.9	0.8	0.3	0.2	
Tb	0.6	0.2	0.4	0.6	0.6	0.1	0.5	0.2	0.1	0.2	0.0	0.3	0.2	0.6	0.2	0.3	0.5	0.2	0.2	0.8	0.6	0.6	0.9	0.7	1.0	0.7	0.9	0.6	1.0	0.6	0.8	0.3	0.2	
Dy	-0.1	0.2	0.7	0.1	-0.1	0.3	0.0	0.3	0.0	0.2	0.0	0.4	0.4	0.3	0.3	0.4	-0.1	0.3	0.3	0.7	0.9	0.9	0.7	1.0	0.7	1.0	0.9	1.0	0.7	1.0	0.9	0.2	0.2	
Ho	0.3	0.1	0.6	0.4	0.3	0.2	0.2	0.2	0.2	0.2	0.0	0.4	0.3	0.4	0.3	0.4	0.2	0.2	0.2	0.8	0.7	0.8	0.8	0.9	0.9	0.9	1.0	0.8	0.9	0.8	0.9	0.2	0.2	
Er	-0.1	0.1	0.7	0.1	-0.1	0.3	0.0	0.3	0.0	0.2	0.0	0.4	0.4	0.3	0.3	0.4	-0.1	0.3	0.2	0.7	0.9	0.9	0.6	0.9	0.6	1.0	0.8	1.0	0.7	1.0	0.9	0.1	0.2	
Tm	0.6	0.1	0.5	0.6	0.6	0.1	0.4	0.2	0.0	0.2	0.0	0.3	0.2	0.5	0.2	0.3	0.5	0.2	0.1	0.7	0.6	0.6	0.8	0.6	1.0	0.7	0.9	1.0	0.7	1.0	0.7	0.8	0.2	0.2
Yb	-0.1	0.2	0.6	0.1	-0.1	0.3	0.0	0.3	0.0	0.2	0.0	0.5	0.4	0.3	0.3	0.4	-0.1	0.3	0.3	0.7	0.8	0.9	0.6	0.9	0.6	1.0	0.8	1.0	0.7	1.0	0.9	0.2	0.2	
Lu	0.2	0.1	0.6	0.2	0.2	0.2	0.2	0.2	0.0	0.2	0.0	0.3	0.4	0.3	0.3	0.4	0.1	0.2	0.2	0.7	0.7	0.8	0.7	0.8	0.8	0.9	0.9	0.9	0.8	0.9	1.0	0.2	0.2	
Th	0.1	0.8	-0.1	0.1	0.1	0.2	0.1	0.0	0.3	0.1	0.1	0.5	0.6	-0.1	0.2	0.1	0.1	0.2	0.2	0.5	0.4	0.3	0.4	0.3	0.3	0.2	0.2	0.1	0.2	0.2	0.2	0.1	0.1	
U	0.0	0.0	0.2	0.1	0.1	0.1	0.1	0.4	0.0	0.1	0.2	0.3	0.1	0.1	0.2	0.1	0.0	0.1	0.2	0.2	0.2	0.2	0.2	0.2	0.2	0.2	0.2	0.2	0.2	0.2	0.2	0.1	1.0	

0.20 weakly correlated 0.30 moderately correlated 0.50 strongly correlated

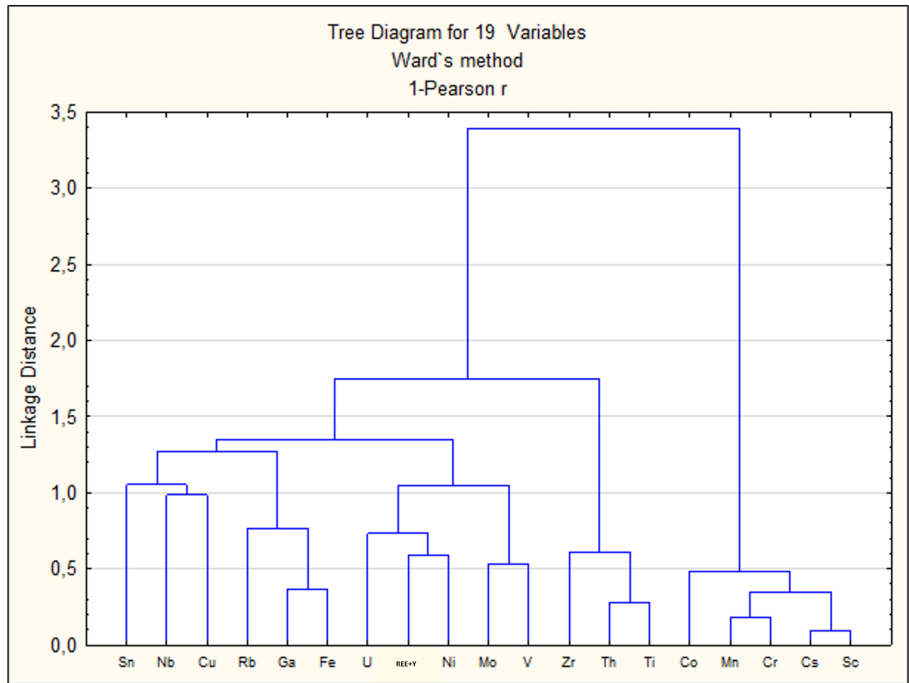


Figure 4. Dendrogram showing the relationship of chemical elements common in metasomatites and skarns

- construction of factor analysis tables (tables 5, 6) and tables of its interpretation (tables 5.1-6.1);

Table 5. Factor analysis table of chemical elements common in carbonaceous-siliceous shales, microquartzites, and quartzites

	Factor 1	Factor 2	Factor 3
Sc	0,6	0,6	-0,1
Ti	0,6	-0,4	0,4
V	0,1	-0,5	-0,5
Cr	0,2	-0,1	-0,7
Mn	0,5	0,5	-0,1
Fe	0,4	-0,5	0,1
Co	0,7	0,4	0,0
Ga	0,7	-0,4	0,2
Rb	0,7	-0,1	0,1
Zr	0,2	-0,5	0,4
Nb	0,6	0,2	0,1
Mo	0,1	-0,4	-0,3
Sn	0,0	0,0	0,1
Cs	0,6	0,6	-0,1
Ba	0,3	-0,5	0,3
Th	0,6	0,1	0,1
U	0,2	-0,2	-0,7
P3Σ+Y	0,3	-0,4	-0,5
Expl.Var	4,126292	2,952331	2,132909
Prp. Totl	0,229238	0,164018	0,118495

Research Article

Table 5.1. Table of classification of chemical elements distributed in carbonaceous-siliceous shales, microquartzites, and quartzites by geochemical associations based on factor analysis and dendrogram

N#F	F+	F-
1	(Sc-Cs)-(Co-Mn)-(Nb-Th)-Fe-(Ti-Ga-Rb)-(Zr-Ba)-Sn-(V-Mo)-(U-REE)-Cr	-
2	(Sc-Cs)-(Co-Mn)-(Nb-Th)	Fe-(Ti-Ga-Rb)-(Zr-Ba)-(V-Mo)-(U-REE)-Cr
3	(Ti-Ga)-(Zr-Ba)-Fe-Rb-Sn-Th	Cr-(U-REE)-(V-Mo)-Mn-Cs

Table 6. Factor analysis table of chemical elements common in metasomatites and skarns

	Factor 1	Factor 2	Factor 3
Sc	0,9	-0,2	0,0
Ti	0,1	0,6	-0,7
V	0,0	0,4	0,6
Cr	0,8	-0,1	0,2
Mn	0,9	-0,2	0,1
Fe	0,1	0,6	0,2
Co	0,8	0,0	-0,1
Ni	0,1	0,5	0,3
Cu	0,1	0,2	-0,1
Ga	0,2	0,7	0,0
Rb	0,2	0,4	0,2
Zr	0,0	0,5	-0,3
Nb	0,1	0,0	-0,3
Mo	0,0	0,4	0,5
Sn	0,0	0,0	-0,1
Cs	0,8	-0,2	0,0
Th	0,2	0,4	-0,7
U	0,1	0,4	0,4
P3Σ+Y	0,1	0,5	0,1
Expl.Var	3,990660	3,008574	2,142206
Prp.Totl	0,210035	0,158346	0,112748

Table 6.1. Table of classification of chemical elements distributed in metasomatites and skarns by geochemical associations based on factor analysis and dendrogram

N#F	F+	F-
1	(Sc-Cs)-(Cr-Mn)-Co	-
2	(Ti-Th-Zr)-(V-Mo)-U-(Ni-REE)-(Fe-Ga)-Cu-Nb-Sn	(Sc-Cs)-(Cr-Mn)-Co-Nb-Sn
3	(V-Mo)-U-(Ni-REE)	(Ti-Th)-Zr-Nb

- by studying the distribution of chemical elements at depth, geochemical associations were distinguished in each section of the main mineralization and a general geochemical model was built. (figures 5);

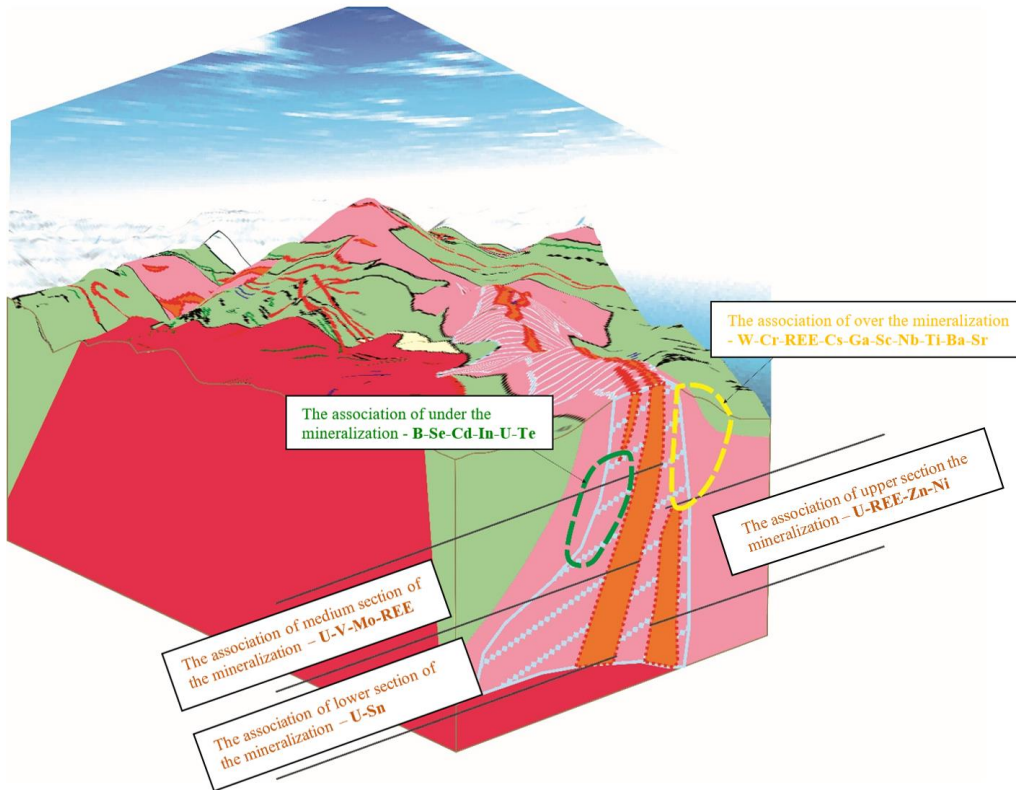


Figure 5. The geochemical model of the distribution of chemical elements in the mineralization zone in a vertical section

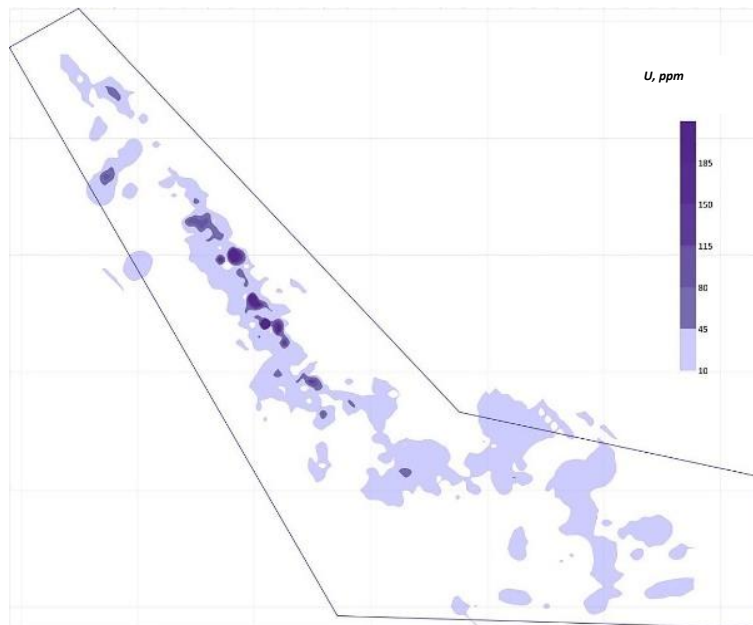


Figure 6. Monoelement map of uranium distribution in the primary halo

Research Article



Figure 7. Additive map of the distribution of rare earth elements and yttrium in the primary halo

CONCLUSION

The black shales of the Northern Nurota ridge, particularly at the Ustuk ore occurrence, demonstrate significant enrichment in uranium, molybdenum, vanadium, and rare earth elements. These enrichments are primarily due to the unique geological and geochemical conditions during the Proterozoic, including high organic content, reducing conditions, and hydrothermal fluid activity. Understanding these factors provides valuable insights for exploring and developing new mineral resources in similar geological settings.

REEs, although typically present in low concentrations, can become enriched in black shales through similar processes of organic binding and hydrothermal input. The specific geochemical behavior of REEs, coupled with the depositional environment of black shales, facilitates their accumulation.

Hydrothermal-metasomatic transformations are important in places where magmatic melts may pass through the boundaries of granitoid massifs and in places where earth faults intersect in different directions. In the Ustuk study area, regional potassium-spar-greisen metasomatism of Upper Carboniferous age is developed, associated with the Ustuk and Sentob granite massifs (Mikhailov V.A.). This factor can be understood as mineralization is predominantly confined to developed metasomatization in carbonaceous-siliceous shales, quartz-sericite (breccia) zones, and in rare cases, skarnization.

Based on the results of a geostatistical study, it has been established that uranium mineralization occurs together with rare earth elements. The fact that geochemical maps of rare earth elements almost ($\approx 70\%$) correspond to uranium halos also confirms their close relationship with each other in mineralization.

Tuyamunite and uraninite occupy the main place among uranium minerals. Sometimes they turn into coffinite and brannerite. Uranium and rare earth elements are rich mainly in iron hydroxides and primary ores - the minerals pyrite, pyrrhotite, molybdenite, and sphene. Rare earth elements are predominantly micro-nano-mineral in size (up to 50-100 microns); they are found mainly in hydroxides and oxides of iron and manganese. The cesium content in them is 7.40-27.12% (Kaneev R.I.).

As a result of the research carried out, the results of previous research were confirmed and the following criteria for geochemical search were developed:

Research Article

- Based on a series of accumulation of chemical elements, it can be concluded that the mineralization of uranium-rare earth elements occurred in quartz-sericite and predominantly carbon-siliceous shales, quartzites, as well as in metasomatites and skarnization zones formed between them.

- Based on the correlation matrix, dendrograms, and tables of factor analysis of chemical elements, the main geochemical associations were established in carbon-silicon shales – (V-Mo)-(U-REE)-Cr and in metasomatites and skarnization - (V-Mo) -U-(Ni-REE).

The research highlights the importance of integrated geochemical studies in uncovering the mineralization processes in black shales and offers practical criteria for future exploration efforts.

REFERENCES

Belov, N.S., Nedoshivin, I.A., & Shvey, I.V. (1965). Assessment of Uranium Potential in the Lower Paleozoic Carbon-Siliceous Formation of the Kyzylkum and Nuratau Mountains. VIMS, Moscow.

Golubev, B.B. (1969). Assessment of Prospects for Discovering Commercial Uranium Deposits in the Paleozoic Carbon-Siliceous Formation of Central Asia. VSEGEI, Leningrad.

Golubev, B.B. (1972). Selection of Areas for Deep Exploration of Uranium Deposits in the Paleozoic Carbon-Siliceous Formation of the Kyzylkum. VSEGEI, Leningrad.

Lukoshchenko, A.P. (1977). Assessment of Uranium Potential in the Carbon-Siliceous Formation of the Auminzatau-Tamditau and Nuratau-Malguzar Mountains with the Compilation of a Prognostic Map at 1:50000 Scale. Tashkent.

Lukoshchenko, A.P. (2000). Conducting Specialized Exploration Work at 1:50000 and 1:25000 Scales to Identify Contrasting Uranium Deposits in Ancient Metamorphic Schists of the Central Kyzylkum. GGP "Kiziltepageologiya," Tashkent.

Lukoshchenko, A.P. (2007). Comparative Characteristics of the Paleozoic Basement of Uranium Ore Regions of the Central Kyzylkum Based on Uranium Potential, Exploration Status, and Technical-Economic Features with a Ranking of Ore Occurrences for Prospective Exploration Work. GP NPC "Urangeologiya," Tashkent.

Rustamov, A.I., & Ergashov, Z.Y. (2016). Specialized Operational Exploration Work to Identify Industrial Uranium Mineralization of Skarn Type within the Ustuk-Fazilman Prospective Area in the Northern Nuratau Mountains. Tashkent.

Turamuratov I.B., Khalilov A.A., Ishboboev T., Ergashov Z.Y., A.A. Kushiev (2020). Three-dimensional geostatistic modeling of hidden uranium-rare-metal-rare-earth mineralization (black shale formations of Western Uzbekistan on the basis of analysis of the spatial distribution of rare rare-earth ore minerals), *PJAE*, 17 (6).